Journal of Cellular Biochemistry 94:126–138 (2005)

Electron Microscopy of DNA Replication in 3-D: Evidence for Similar-Sized Replication Foci Throughout S-Phase

Karel Koberna,[1,2] Anna Ligasová,[1,2] Jan Malínský,[1,2] Artem Pliss,[3] Alan J. Siegel,[3] Zuzana Cvačková,[1,2] Helena Fidlerová,[1,2] Martin Mašata,[1,2] Markéta Fialová,[1,2] Ivan Raška,[1,2] and Ronald Berezney[3]*

[1]Department of Cell Biology, Institute of Experimental Medicine,
Academy of Sciences of the Czech Republic, Albertov 4, CZ-12800 Prague 2, Czech Republic
[2]Institute of Cellular Biology and Pathology, 1st Faculty of Medicine, Charles University, Albertov 4,
CZ-12800 Prague 2, Czech Republic
[3]Department of Biological Sciences, State University of New York at Buffalo, Buffalo, New York 14260

Abstract DNA replication sites (RS) in synchronized HeLa cells have been studied at the electron microscopic level. Using an improved method for detection following the in vivo incorporation of biotin-16-deoxyuridine triphosphate, discrete RS, or foci are observed throughout the S-phase. In particular, the much larger RS or foci typically observed by fluorescence microscopic approaches in mid- and late-S-phase, are found to be composed of smaller discrete foci that are virtually identical in size to the RS observed in early-S-phase. Pulse-chase experiments demonstrate that the RS of early-S-phase are maintained when chased through S-phase and into the next cell generation. Stereologic analysis demonstrates that the relative number of smaller sized foci present at a given time remains constant from early through mid-S-phase with only a slight decrease in late-S-phase. 3-D reconstruction of serial sections reveals a network-like organization of the RS in early-S-phase and confirms that numerous smaller-sized replication foci comprise the larger RS characteristic of late-S-phase. J. Cell. Biochem. 94: 126–138, 2005.

Key words: mammalian DNA replication; replication foci; S-phase; cell nucleus; chromatin; electron microscopy; immunogold labeling

Considerable progress has been made in studying replication sites (RS) or foci in mammalian cells using fluorescence microscopy and computer imaging approaches. Characteristic patterns of RS are observed in early-, mid-, and late-S-phase that serve as indicators for each of these S-phase periods [Nakamura et al., 1986; Nakayasu and Berezney, 1989; van Dierendonck et al., 1989; Mazzotti et al., 1990; Fox et al., 1991; Kill et al., 1991; Manders et al., 1992; Neri et al., 1992; O'Keefe et al., 1992; Sparvoli et al., 1994; Ferreira et al., 1997; Somanathan et al., 2001; Dimitrova and Berezney, 2002]. The changes in the spatial and temporal organization of these RS are believed to reflect the choreography for the DNA replication program that proceeds from copying transcriptionally active euchromatic DNA in early-S to relatively inactive heterochromatic DNA later in S-phase [Ma et al., 1998]. These studies have led to models in which the individual RS of early-S-phase are proposed to be

This paper is dedicated to the memory of Professor Zdenek Lojda.

Abbreviations used: RS, DNA replication site(s); PCNA, proliferating cell nuclear antigen; biotin-16-dUTP, biotin-16-deoxyuridine triphosphate; BrdU, 5-bromo-5′-deoxyuridine; EM, electron microscopy; dT, 2′-deoxythymidine.

Grant sponsor: National Institutes of Health (to RB); Grant number: R01 GM072131-23; Grant sponsor: Grant Agency of the Czech Republic (to KK); Grant number: 304/01/0729; Grant sponsor: Grant Agency of the Czech Republic (to JM); Grant number: 304/03/1121; Grant sponsor: Grant Agency of the Czech Republic (to IR); Grant numbers: 304/04/0692, 304/02/0342; Grant sponsor: Grant Agency of the Czech Academy of Sciences (to IR); Grant number: IAA5039103; Grant sponsor: Ministry of Education, Youth, and Sports (to IR); Grant number: MSM111100003; Grant sponsor: Ministry of Education, Youth, and Sports (to AL); Grant number: FRVS202826 G989.

*Correspondence to: Ronald Berezney, Department of Biological Sciences, State University of New York at Buffalo, Buffalo, NY 14260. E-mail: berezney@buffalo.edu

Received 29 July 2004; Accepted 30 July 2004

DOI 10.1002/jcb.20300

composed of multiple replicons (chromatin loops) with an average DNA content of ~1 Mbp [Nakamura et al., 1986; Jackson and Pombo, 1998; Ma et al., 1998; Berezney et al., 2000; Berezney, 2002]. The persistence of these labeled sites throughout the cell cycle and into subsequent cell generations has led to the further view that the early-S RS are fundamental higher order domains of chromatin organization and function [Jackson and Pombo, 1998; Ma et al., 1998; Zink et al., 1998; Berezney, 2002].

In contrast to the RS of early-S-phase, our understanding of the organization of chromatin in RS of mid- and late-S-phases is much more limited. A major difficulty is that many of these RS are much larger in size as they correspond to heterochromatin regions replicated in these later periods of S-phase. While it is commonly assumed that these larger foci are composed of multiple units or chromatin domains of replication of similar size to the RS of early-S-phase, data supporting this possibility is limited [Nakayasu and Berezney, 1989; Raska et al., 1989, 1991; Leonhardt et al., 2000].

Electron microscopic analysis provides an enormous increase in resolution to overcome imaging limitations of the light microscope and to enable a more accurate and detailed understanding of replication site organization in the cell nucleus. Surprisingly, however, high resolution electron microscopic studies have to date not contributed significantly [with the exception of the earlier observations of Raska et al., 1989, 1991] to our understanding of the numerous replication foci detected in early-S-phase and the much larger but more limited number of foci characteristic of late-S-phase [Mazzotti et al., 1990; Rizzoli et al., 1992; Hozak et al., 1993, 1994; Jaunin et al., 2000]. Since a major difficulty with this approach is the relatively weak labeling patterns typically obtained following short pulses with bromodeoxyuridine, we have taken steps in this study to improve the signal intensity for thin sectioning electron microscopic analysis. Intense labeling for DNA replication is observed that is concentrated at discrete sites throughout S-phase. The typically larger RS or foci observed by fluorescence microscopy in mid- and late-S-phase are found to be composed of smaller discrete replication foci virtually identical in size to the RS of early-S-phase. Pulse-chase studies reveal that the smaller foci of early-S are maintained throughout the S-phase and into the subsequent cell generation. Moreover, the relative number of smaller RS present at a given time does not drastically change during S-phase progression. 3-D reconstruction of serial sections demonstrates a higher order arrangement of the early-S-phase replication foci into network-like arrays and confirms that the small replication foci of late-S-phase are tightly compacted into the characteristic larger RS or foci.

MATERIALS AND METHODS

Cell Culture and Synchronization

HeLa cells were grown either in flasks or on circular coverslips in Petri dishes and cultured in Dulbecco's modified Eagle's medium (DMEM) supplemented with 10% fetal calf serum (Sigma-Aldrich, Steinheim, Germany), 1% glutamine, 1% penicillin, 1% streptomycin, and 0.85 g/L $NaHCO_3$ at 37°C in a humidified atmosphere containing 5% CO_2. Synchronization at the G_1/S border was achieved by a double 2′-deoxythymidine block (dT; Sigma, St. Louis, MO). The cells were incubated in DMEM containing 3 mM dT for 16 h, then in a fresh medium for 12 h and again for 16 h in a medium with 3 mM dT. After 100 min incubation in a normal medium, more than 90% of the cell population started DNA synthesis as judged by immunocytochemistry. Nine hours later cells exited S-phase as more than 95% of them did not incorporate the 5-bromo-5′-deoxyuridine (BrdU).

Labeling of Newly Synthesized DNA

BrdU (Sigma Chemicals Co.) or biotin-16-deoxyuridine triphosphate (biotin-16-dUTP) (Roche Diagnostics GmbH, Penzberg, Germany) were used as markers of newly synthesized DNA. If BrdU was used, cells were incubated in medium containing 20 μM BrdU in 5% CO_2 at 37°C for 10 min and processed for light or electron microscopy. Biotin-16-dUTP was delivered into cells with a hypotonic shift procedure [Koberna et al., 1999]. HeLa cells were quickly rinsed in pre-warmed KHB buffer (30 mM KCl, 10 mM HEPES pH 7.4), then overlaid with KHB containing 0.2 mM biotin-16-dUTP, incubated in a humidified chamber at 37°C for 5 min, washed, incubated in medium in 5% CO_2 at 37°C for 10 or 3 min and processed for light or electron microscopy. Importantly, the biotin-16-dUTP is efficiently incorporated into DNA of

cells for 15–20 min as determined from fluorescence intensity measurements (data not shown). In the case of pulse-chase-pulse experiments, BrdU and biotin-16-dUTP were used as replication markers. After the first pulse, the remaining BrdU was washed out by medium containing 100 μM thymidine. Cells were viewed using the Olympus Provis or Leica TCS NT microscope. The images were captured by a charge-coupled device camera (PXL with KAF 1400 chip; Photometrics, Ottobrunn, Germany) running on IPLab Spectrum or AnalySIS softwares. We avoided multinuclear cells as well as cells with large nuclei possessing apparently highly elevated genome copies, which were occasionally seen in the culture.

Antibodies

Mouse anti-bromodeoxyuridine antibody (Roche Diagnostics GmbH) and rabbit anti-biotin antibody (Enzo, New York, NY) were used as primary antibodies. The secondary anti-mouse and anti-rabbit antibodies conjugated with FITC, Cy3, or 6 nm or ultra-small grade gold particles, were kindly donated by Jackson ImmunoResearch Laboratories.

Electron Microscopy

If not stated otherwise, synchronized cells were used in all the electron microscopic studies. HeLa cells with incorporated BrdU were fixed in 8% formaldehyde in 0.2 M pipes, pH 6.95 for 12 h, washed in PBS, dehydrated in methanol and propyleneoxide and embedded in Epon (Fluka Chemie GmbH). Ultrathin sections were cut, incubated with anti-bromodeoxyuridine antibody, washed in PBS, incubated with 6 nm gold anti-mouse adduct, washed in water and air-dried.

The ultrastructural mapping of newly synthesized biotin-16-dUTP labeled DNA was achieved using a pre-embedding approach. The cells were fixed in 2% formaldehyde in PBS for 10 min, washed in PBS, treated for two min each in 30, 50, 70, 90, 70, 50, and 30% ice-cold methanol and washed in PBS. Prior to immunolabeling, the cells were treated with 0.05 M glycine in PBS and then in 0.5% BSA for the blocking of unspecific binding. Biotinylated DNA was visualized with an anti-biotin antibody followed by an anti-rabbit ultrasmall gold adduct. The silver intensification was performed according to Danscher [1981]. Finally, the cells were post-fixed in 8% formaldehyde and dehydrated in gradually increasing methanol concentrations and propyleneoxide, and embedded in epon or lowicryl. Ultrathin epon and lowicryl sections were cut on a Reichert Ultracut E microtome with a Diatome diamond knife (Diatome Ltd.). The sections were stained with uranyl acetate and viewed using a Jeol 1200 EX or Zeiss EM 900 electron microscope equipped with MegaView II camera. The evaluation of gold labeling was performed using analySIS software (Soft Imaging System GmbH, Münster, Germany).

3-D Reconstruction and Stereological Analysis

Prints of electron micrographs from serially sectioned nuclei were aligned into a stack of images by registering contiguous features from adjacent sections. After alignment, a region of interest was cut from the stack and each section was scanned. Labeled sites were selected either by manual contour mapping or computer segmentation using IPLab software (Scanalytics, Fairfax, VA). For 3D reconstruction, the stacks of either pseudocolored segments or contours were projected in 3-D with IPLab software. Anaglyphs were prepared using two images from the 3-D projection series which were rotated 10° relative to one another.

The size of replication domains was estimated as follows: the most external gold (silver) particles were joined by straight lines given rise to a polygon. The maximum diameter and area of these polygons were measured. 300 RS were analyzed for each period of S-phase for three separate experiments. Only sites containing four or more gold particles were taken into account.

The ratio (R_E:R_M:R_L) of relative nuclear volumes occupied by RS in early-, mid-, and late-S-phase cells was calculated as the ratio of relative nuclear areas occupied by RS. The square lattice of regularly spaced points was used for area estimation [Gundersen et al., 1988]. Thirty images of nuclear profiles from three independent experiments were evaluated for every S-phase stage. The value of R_E was set to 1.00.

The ratio of nuclear volumes of cells in early-, mid-, and late-S phase was estimated from stacks of confocal images. Cells were labeled with the DNA-specific dye YOYO-1 or with anti lamin A/C antibody and 3-D stacks of confocal images with the sampling $50 \times 50 \times 300$ nm were acquired. The total area of all sections was

calculated for 20 nuclei in every S-phase stage. If not stated otherwise, cells incorporating biotin-16-dUTP were used for all the stereological evaluations.

RESULTS

Kinetic Studies of Fluorescent Replication Patterns During S-Phase

Numerous studies using BrdU or biotinylated deoxyuridine incorporation and fluorescence microscopy have demonstrated three major types of replication site or foci patterns in a variety of mammalian cell lines (Fig. 1) corresponding to early (type I), mid (type II), and late (type III) stages of S-phase [Nakayasu and Berezney, 1989; van Dierendonck et al., 1989; Mazzotti et al., 1990; Fox et al., 1991; Kill et al., 1991; Manders et al., 1992; Neri et al., 1992; O'Keefe et al., 1992; Sparvoli et al., 1994; Ferreira et al., 1997; Somanathan et al., 2001; Dimitrova and Berezney, 2002]. While some studies have identified five different patterns of foci, these correspond to further subdivision of the three basic types [Dimitrova and Berezney, 2002]. As background for a comprehensive study of these replication patterns and the foci that compose them at the electron microscopic level, an analysis of the S-phase and the corresponding replication site patterns was performed in HeLa cells grown in monolayer. In an initial control, we demonstrated that a 10 min in vivo pulse of BrdU or biotin-16-dUTP had no effect on the doubling time of the HeLa cells (~24 h). The average length of S-phase in this cell line was estimated by means of a dual labeling pulse-chase-pulse experiment as described in Materials and Methods. An asynchronous cell population was labeled with BrdU for 10 min, chased in cultured medium without BrdU for 5, 6, 7, 8, 9, or 10 h followed by in vivo labeling with biotin-16-dUTP for 10 min after hypotonic shift (see Materials and Methods). Data from 900 cells from three independent experiments demonstrated that 16, 10, 7, 3, and 0% of cells exhibited two color signals following 5, 6, 7, 8, and 9 or 10 h chase periods, respectively. We conclude that the average S-phase duration is approximately 9 h. This was further supported by single labeling experiments with BrdU in asynchronously dividing HeLa cells. Approximately 38% of cells exhibited a replication signal after 10 min incubation with BrdU (results not shown).

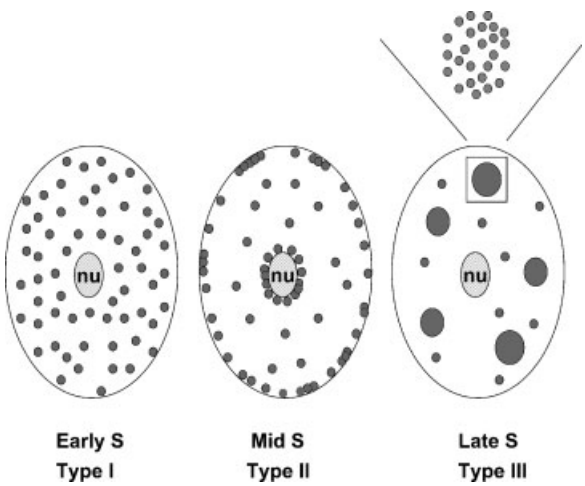

Fig. 1. The three main types of replication site patterns in the mammalian cell nucleus are composed of similarly sized foci. Type I (early-S) patterns consist of numerous foci distributed throughout the nuclear interior. In type II (mid-S) patterns, the replication foci are predominantly of similar size as in early-S-phase and are concentrated along the nuclear and nucleolar borders in association with heterochromatin. Some foci, however, appear larger than those in early-S-phase due to the tight packing of the individual foci over heterochromatic regions along the periphery of the nucleus and nucleolus. Type III (late-S) patterns are composed of much larger replication foci distributed over the late replicating heterochromatinic regions. As demonstrated in this study, these larger foci are comprised of numerous smaller replication foci that are identical in size to the replication sites (RS) observed in early-S-phase. This is illustrated for the replication site in the boxed area. nu, nucleolus.

Next, we determined the temporal order and length of the replication site patterns that appear during the progression of S-phase. Following a single 10 min pulse with BrdU, the typical five patterns of RS were identified [Dimitrova and Berezney, 2002] corresponding to a large number of small foci in early-S (types IA and IB), foci concentrated along the periphery of the nucleus and nucleoli characteristic of mid-S (type II) and larger foci over heterochromatin domains in late-S-phase (types IIIA and IIIB) Using a double labeling pulse-chase-pulse experiment (see Materials and Methods), we estimated the approximate time for each replication pattern as 3.9 h for type I (early-S), 3.4 h for type II (mid-S), and 1.7 h for type III (late-S).

To confirm the temporal order of these replication patterns, we performed experiments with HeLa cells synchronized at the G_1/S border with a double thymidine block (see Materials and Methods). Previous studies have demonstrated that this synchronization method did not affect the timing and organization of the

replication patterns [Malinsky et al., 2001]. We found that 90% of the cells exhibited the early-S replication pattern 100 min after release from the thymidine block. After an additional 4 and 7 h, most of the cells exhibited mid- and late-S-phase patterns, respectively. This timing of replication patterns matched well our results in asynchronous cells and led us to conclude that we could use this synchronization procedure to accurately examine, by electron microscopy, the replication foci in early-, mid-, and late-S-phases.

Identification of DNA Replication Sites (RS) Following High Resolution Electron Microscopic Immunogold Labeling

As a first step in examining the organization of RS at the electron microscopic level, HeLa cells synchronized by the double thymidine block procedure were processed for post-embedding immunogold labeling during early-S-phase (100 min after release), mid-S-phase (340 min after release), and late-S-phase (520 min after release). Typical results are shown in Figure 2A–C. While the gold particles observed during early- and mid-S-phase are typically clustered into small regions that could correspond to discrete RS or foci (Fig. 2A,B, insets), the relatively weak labeling resulted in significant distances between many of the gold particles. This makes it difficult to estimate the size and borders of these presumptive clusters. Similarly, the gold particles observed in late-S-phase were often grouped together into small clusters, but the relatively large distances between many of the particles, made it difficult to determine how these small clusters might be arranged into the larger foci characteristic of late-S-phase (Fig. 2C, inset). Indeed, determining where one cluster ends and another one begins was a challenging task.

These findings led us to develop a more sensitive approach for labeling RS at the electron microsopic level. We reasoned that a significant increase in the number of gold particles decorating the RS would enable a more accurate identification and evaluation of these individual sites. Three major changes in conditions were adapted to enhance the sensitivity of immunogold labeling (see Materials and Methods). First, rather than incorporation of BrdU, a hypotonic shift method [Koberna et al., 1999] was used to incorporate biotin-16-dUTP label directly into living cells. Secondly, the samples were processed for immunogold labeling before embedding (pre-embedding) rather than post-embedding. This enabled immunogold labeling to occur through the fixed cell sample rather than on a single thin section embedded in the plastic resin. Lastly, silver enhancement was used to increase the signal intensity of the gold particles.

Use of this improved pre-embedding protocol resulted in a striking enhancement in the signal intensity over individual RS. Discrete clusters of closely spaced gold particles of high intensity were now typically observed that resembled replication foci in early-, mid-, and late-S-phase (Fig. 2D–F). At higher magnification (see insets to Fig. 2D–F) these sites appear to be similar in size throughout S-phase. While the individually labeled gold clusters in early-S-phase are generally at a distance (>0.2 μm) that would enable their resolution as separate foci by fluorescence microscopy (Fig. 2D, inset), this is not the case for late-S (or in some instances mid-S patterns) where discrete clusters are observed within a 0.1 μm distance of each other (Fig. 2E,F, insets). These findings suggest that the larger foci observed in late- and mid-S-phase by fluorescence microscopy, are composed of smaller foci. The smaller foci are resolvable at the electron microscopic level and appear to be similar in size to the replication foci observed in early-S-phase.

This prompted us to determine the size of the individual gold clusters following the 10 min labeling period. Three hundred measurements from 30 different nuclei and three separate pre-embedding experiments were performed on gold clusters from each of the three periods of S-phase. The average area occupied by individual clusters in early-, mid-, and late-S-phase was strikingly similar (4,515, 4,650, and 4,625 nm^2, respectively) as were the frequency distributions of area for each period of S-phase (Fig. 3A,C). Consistent with the area measurements, the average size of individual clusters based on the diameter was nearly identical (110, 120, and 110 nm) in early-, mid-, and late-S-phase, respectively, as were the corresponding frequency distributions of measured diameters (Fig. 3B,D). These data demonstrate that the size of the gold clusters, and the individual replication foci that they represent, do not change significantly during S-phase. Moreover, they are in accordance with our measurements of RS in non-synchronized cells. The average area of individual RS in non-synchronized cells

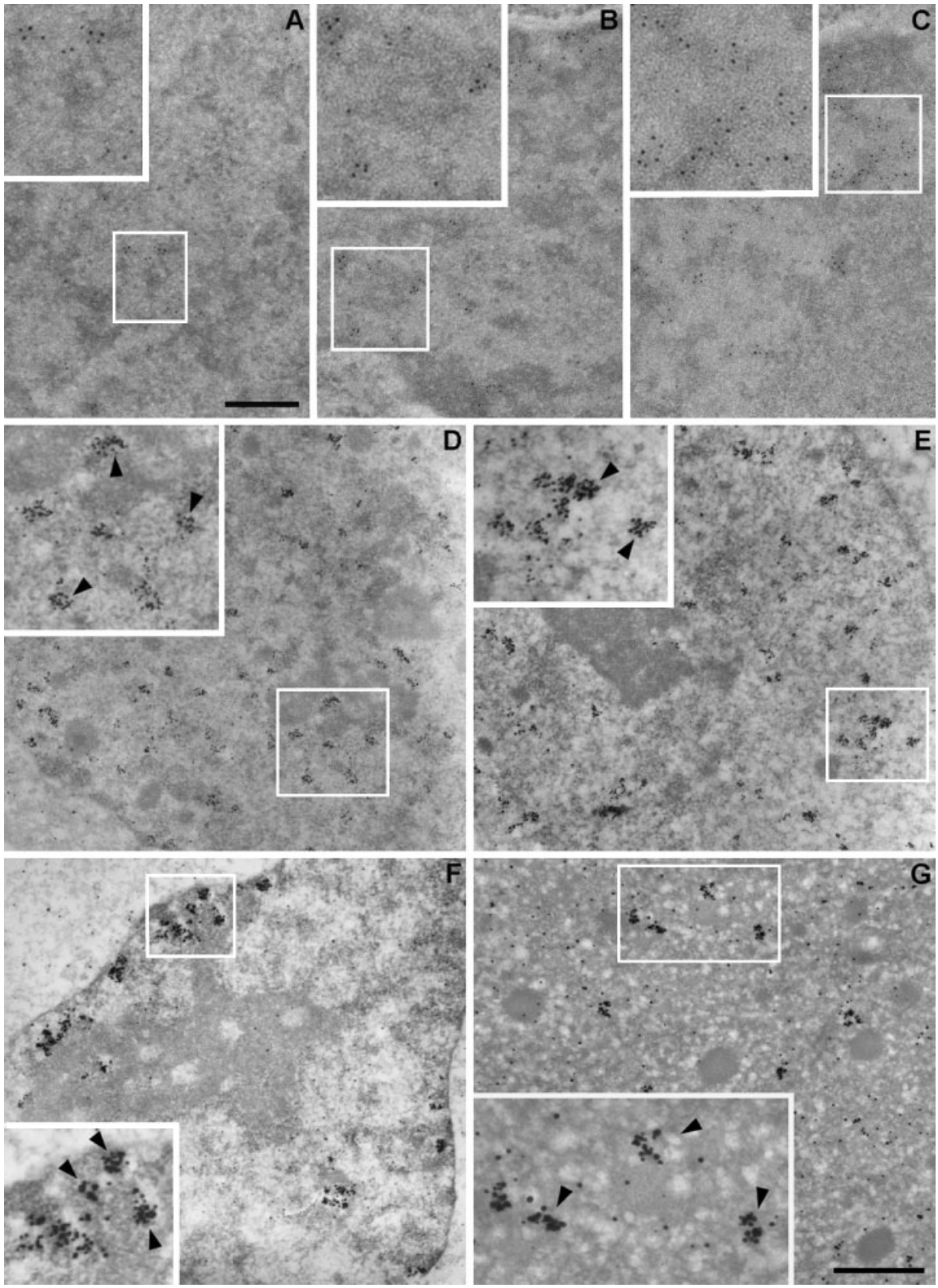

Fig. 2. Electron microscopy mapping of RS on thin sections of HeLa cells. Cells were either labeled with 5-bromo-5′-deoxyuridine (BrdU) (**A**–**C**: post-embedding detection), or with biotin-16-deoxyuridine triphosphate (biotin-16-dUTP) (**D**–**G**: pre-embedding detection). Cells were synchronized in early (A, D, G), mid (B, E), and late (C, F) S-phase. Groups of gold particles decorating small foci were observed after 10 min of labeling (insets to D–F). Several such foci were sometimes clustered in mid-S and frequently in late-S-phase (E, F, and insets). Similarly sized foci were observed after 3 min labeling pulse (G and inset). Bar: 1 μm. Insets are 2× magnified.

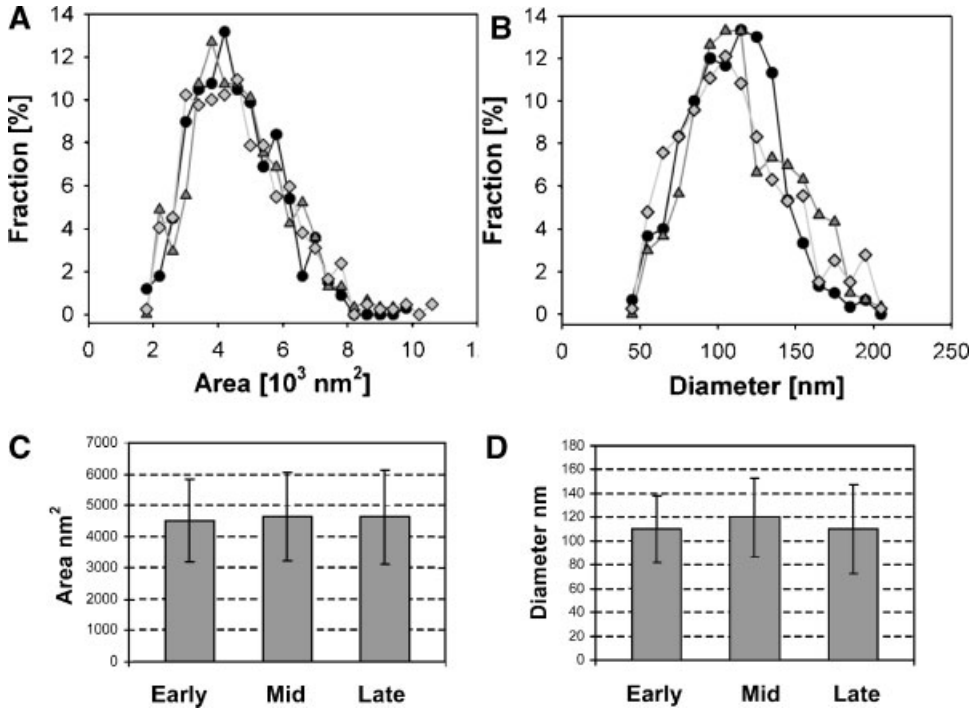

Fig. 3. Quantitative analysis of replication foci size during S-phase. The total distribution of replication foci in terms of area (**A**) and diameter (**B**) of individual foci are plotted for early-S (circles), mid-S (triangles), and late-S (diamonds). **C** and **D** show the average areas and diameters, respectively, for early-, mid-, and late-S-phase replication foci. Error bars correspond to 1 standard deviation.

was 4,605 nm^2 and thus matched the sizes found throughout S-phase in synchronized cells.

Previous fluorescent microscopic studies demonstrated that the replication foci in early-S-phase do not significantly change their size in pulse periods ranging from 2 to 30 min [Ma et al., 1998]. Similarly, we compared the size of RS of early-S-phase labeled with biotin-16-dUTP for 3 versus 10 min. The average area of replication clusters was strikingly similar ($4{,}550 \pm 1{,}300$ and $4{,}345 \pm 1{,}220$ nm^2) for 10 and 3 min labeling intervals, respectively. It is likely that this small difference in area size is a result of the much lower labeling density of RS following the 3 min versus the 10 min pulse (data not shown) rather than to a real change in the size of replication foci.

Replication Foci Labeled in Early-S-Phase Persist as Similarly Labeled Sites Throughout S-Phase and Into the Next Cell Generation

Studies at the fluorescent microscopic level have demonstrated that the replication foci labeled in early-S-phase, are maintained as identically-looking labeled foci throughout the S-phase and into subsequent cell generations [Sparvoli et al., 1994; Jackson and Pombo, 1998; Ma et al., 1998; Zink et al., 1998]. These findings have contributed to the current view that the early-S-phase replication foci represent fundamental units of higher order chromatin domains [Jackson and Pombo, 1998; Ma et al., 1998; Zink et al., 1998; Berezney, 2002]. If the gold clusters that we have visualized in our microscopic analysis correspond to these early-S-phase replication foci, they should also persist as similar clusters in subsequent cell generations. To address this issue, HeLa cells synchronized in early-S-phase were pulsed for 10 min with biotin-16-dUTP and chased for 4 h into a later stage of S-phase or for 18 h into the G_1-phase of the next cell generation. In both cases, clusters of gold particles were observed scattered throughout the extranucleolar regions of the nucleus in patterns very similar to corresponding gold clusters observed during early-S-phase (Fig. 4).

Calculating the Relative Number of Small RS During S-Phase Progression

Using stereologic analysis and assuming that the average size of the small replication foci are

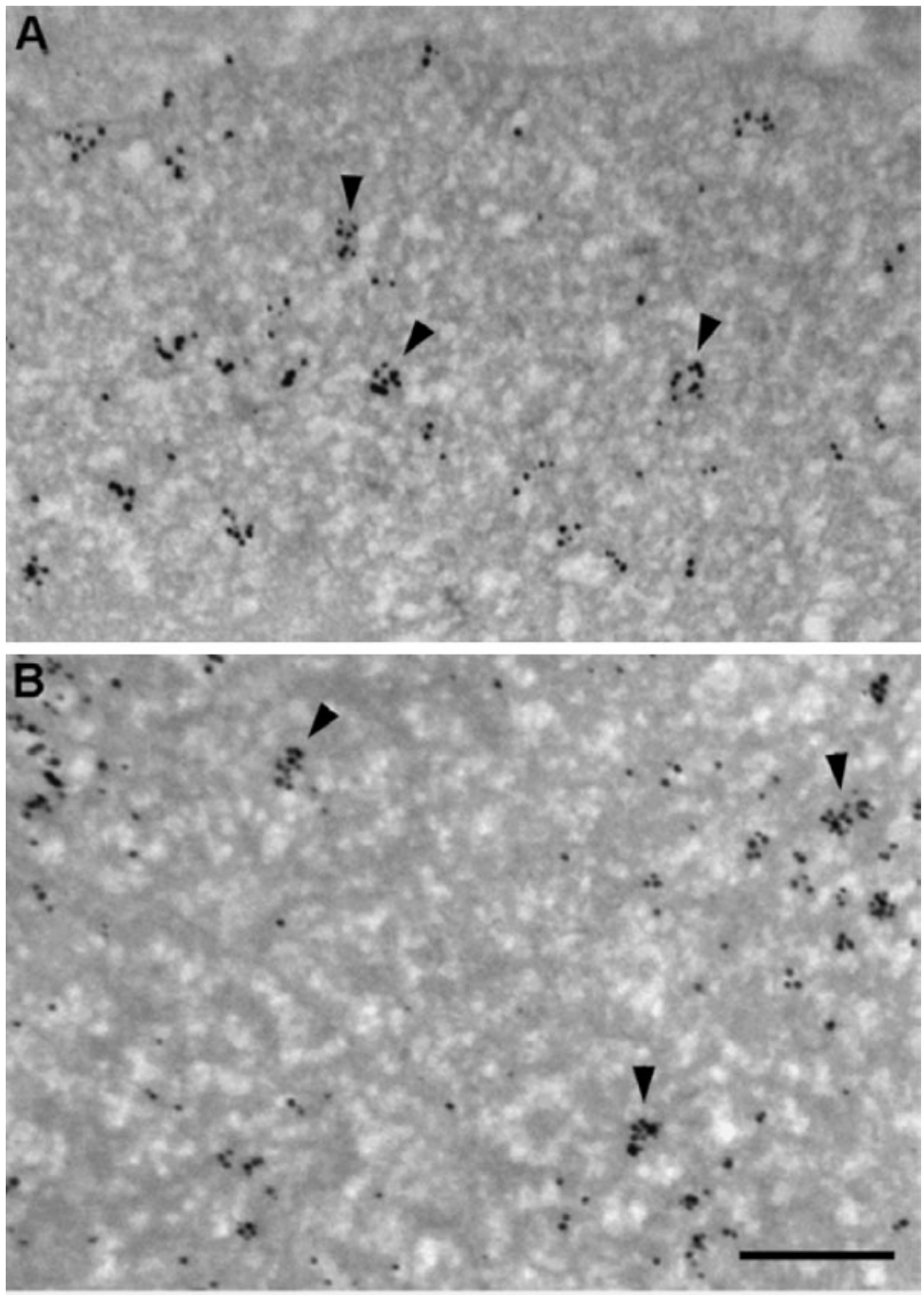

Fig. 4. Electron microscopy mapping of chromatin domains previously labeled in early-S-phase. Cells were synchronized in early-S-phase, labeled for 10 min with biotin-16-dUTP and chased for 4 h (**A**) or 18 h (**B**). Groups of gold particles decorate small chromatin domains in both images that are similar to the replication foci labeled in early-S-phase (see Fig. 2). Bar: 500 nm.

virtually the same throughout S-phase, we estimated the relative number of small RS present at a given time in S-phase. First, we determined the ratio of relative nuclear volumes occupied by the total RS present on an average in early-, mid-, and late-S-phases (see Materials and Methods). For the pre-embedding approach, this ratio was approximately 1.00, 0.93, and 0.54 for early-, mid-, and late-S-phase cells, respectively. Importantly, data derived from

BrdU labeled cells (post-embedding approach) provided similar results: 1.00, 0.92, and 0.62, respectively. As the pre-embedding approach enabled clearer resolution of replication foci (compare Fig. 2A–G), only data derived from this method were used for further analysis.

Since during S-phase progression, the nuclear volume increases [Fidorra et al., 1981], the relative volumes occupied by RS needed to be normalized to the relative nuclear volumes in early-, mid-, and late-S-phase cells, respectively. Using confocal microscopy (see Materials and Methods), we determined the ratios of total nuclear volumes to be 1.00 (early-S), 1.09 (mid-S), and 1.28 (late-S), respectively. Next, we calculated the relative number of RS as a product of the relative volume occupied by RS and the relative nuclear volume and obtained values of 1.00 (early-S), 1.01 (mid-S), and 0.79 (late-S). Our analysis, therefore, indicates that the relative number of active small RS at anytime during S-phase is approximately constant with a small decrease (~20%) during late-S-phase.

3-D Reconstruction of RS From Electron Microscopic Serial Sections

Serial sections from cells labeled at early- and late-S-phase were processed for 3-D reconstruction (see Materials and Methods). Briefly, the serial sections were aligned and projected in 3-D for direct observation as anaglyphs. In early-S-phase, the gold clusters corresponding to individual replication foci are arranged three-dimensionally into higher order arrays that form a network-like organization (Fig. 5E). Contour mapping of the gold clusters was then performed on the individual sections (Fig. 5A–D), followed by 3-D reconstruction of the contours at each section. Consistent with the analysis of the gold labeled sites (Fig. 5E), the contours form higher order arrays that resemble network-like structure (Fig. 5F).

In late-S-phase, the smaller clusters of gold particles that compose the much larger replication foci merge together in 3-D (Fig. 6E). Contour mapping of the individual gold clusters at each section (Fig. 6A–D) followed by 3-D reconstruction, demonstrates the large number of contours that typically compose the larger replication foci of late-S-phase (Fig. 6F). The number of contours at these large late-S-phase replication foci ranged—in correspondence to the size of the foci—from <10 to >75.

DISCUSSION

Fluorescent microscopic studies of DNA RS or foci have contributed strikingly to our understanding of the structural organization of DNA replication in mammalian cells. As the cell progresses through S-phase, distinct patterns of these RS are observed that are characteristic of early-, mid-, and late-S-phases [Fig. 1 and Nakayasu and Berezney, 1989; van Dierendonck et al., 1989; Mazzotti et al., 1990; Fox et al., 1991; Kill et al., 1991; Manders et al., 1992; Neri et al., 1992; O'Keefe et al., 1992; Sparvoli et al., 1994; Ferreira et al., 1997; Somanathan et al., 2001; Dimitrova and Berezney, 2002]. More detailed studies including three-dimensional fluorescence microscopy and computer image analysis have led to current models of RS as discrete chromatin domains containing an average of ~1 Mbp of DNA [Nakamura et al., 1986; Jackson and Pombo, 1998; Ma et al., 1998; Berezney et al., 2000; Berezney, 2002]. One assumption of these models is that the chromatin domains measured in early-S-phase are also the basic units for replication in the later stages of S-phase. The larger replication foci that are observed in mid- and late-S-phase are interpreted as being comprised of numerous RS of similar size as the early-S sites [see Fig. 1 and Nakayasu and Berezney, 1989]. Since the larger foci typically correspond to heterochromatic region, it is a reasonable assumption that the much higher compaction of chromatin in these regions makes it difficult to visualize the individual smaller RS that might comprise the larger foci. While studies involving GFP expression of the major replicational factor proliferating cell nuclear antigen (PCNA) provide evidence for this possibility [Leonhardt et al., 2000], these observations are limited in both scope and by the resolution of light microscopy.

A number of previous electron microscopic studies using colloidal gold labeling, have suggested that the RS are organized into clusters that might correspond to the replication foci observed in early-S-phase and the larger foci observed in late-S-phase by fluorescence microscopy [Raska et al., 1989, 1991; Mazzotti et al., 1990; Rizzoli et al., 1992]. These previous studies, however, are typically limited by the relatively weak labeling obtained using traditional post-embedding protocols. This results in relatively large distances between individual gold particles and a corresponding difficulty in

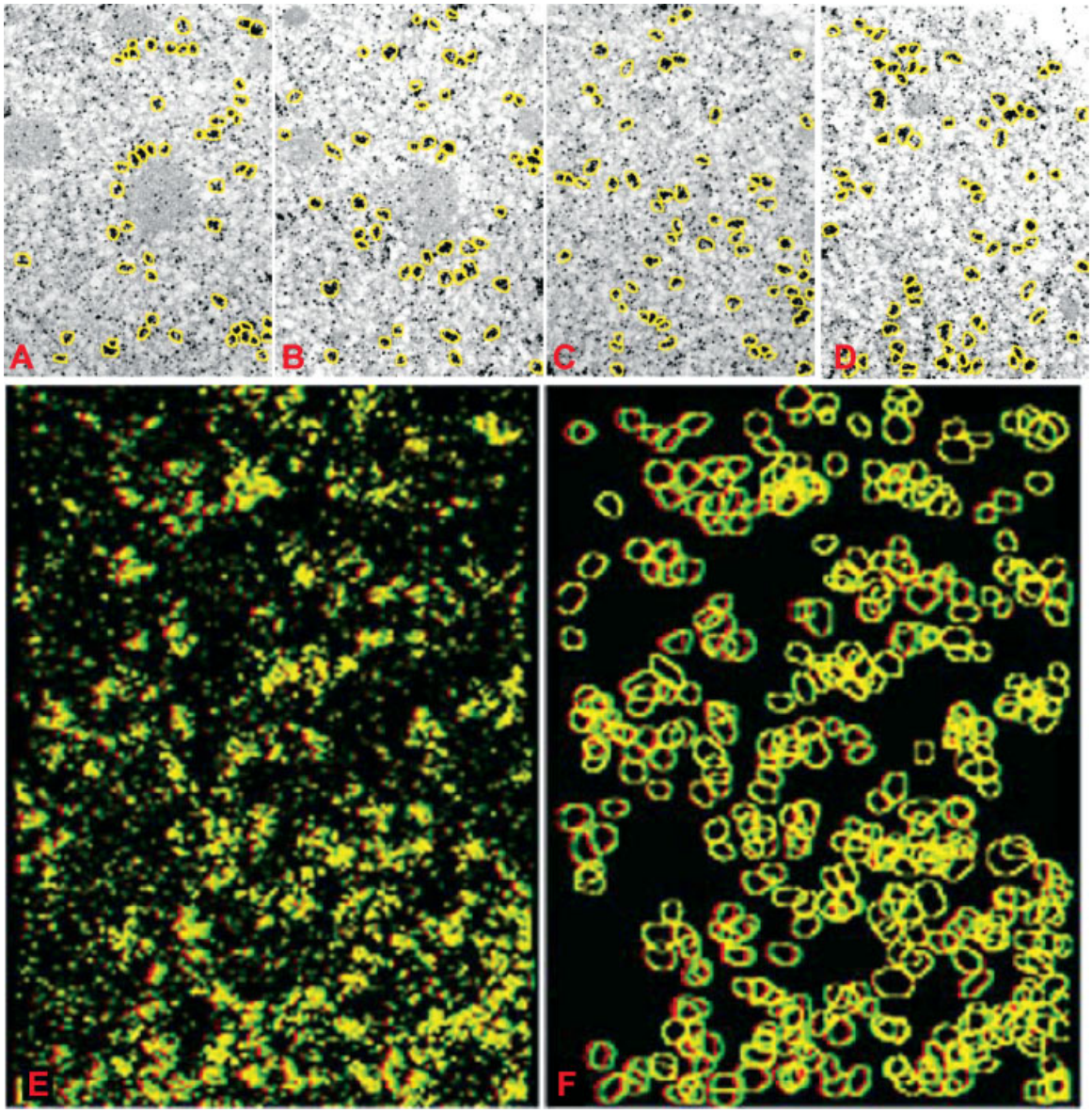

Fig. 5. Three-dimensional visualization of RS in early-S-phase. Images of seven consecutive serial sections of early-S-phase labeled replication foci were aligned using ultrastructural markers common to adjacent sections (see Materials and Methods). **Panels A–D** show four representative sections in which the replication foci are outlined with yellow contours. Black field anaglyphs of the 3-D reconstructions are shown for the computer segmented replication foci (pseudo-colored in yellow, **panel E**) and for contours (yellow) outlining the replication foci (**panel F**). The images of panels E and F can be observed in 3-D with red/blue-green viewers.

accurately assigning individual gold particles to higher order clusters (see Fig. 2A–C). While larger regions of gold particles are typically observed in late-S-phase that likely correspond to the larger foci identified by fluorescence microscopy, the limited labeling has made it difficult to resolve the smaller foci that might comprise the larger labeled regions. Immunogold labeling for PCNA, however, has provided some evidence for smaller clusters of replicative activity within the larger replication foci of late-S-phase [Raska et al., 1989].

To circumvent these technical difficulties, we have developed a highly sensitive electron microscopy (EM) localization procedure for RS involving direct in vivo incorporation of biotin-16-dUTP followed by labeling with colloidal gold particles and silver enhancement before embedding of the specimens (pre-embedding) for electron microscopy. Under these conditions,

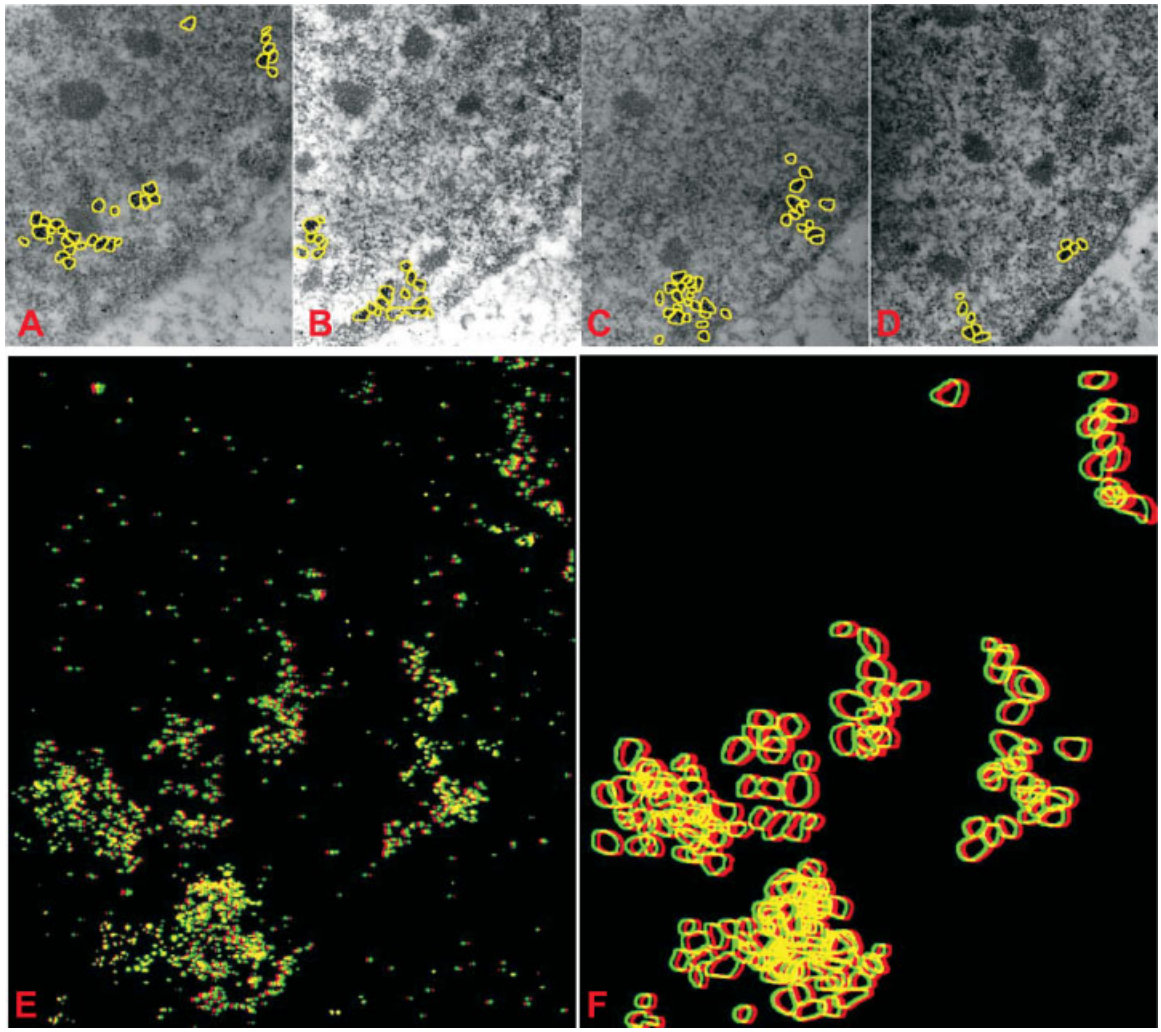

Fig. 6. Three-dimensional visualization of RS in late-S-phase. Images of nine consecutive serial sections of late-S-phase labeled replication foci were aligned using ultrastructural markers common to adjacent sections (see Materials and Methods). **Panels A–D** show four representative sections in which the small replication foci within the larger-sized foci of late-S-phase are outlined with yellow contours. Black field anaglyphs of the 3-D reconstructions are shown for the computer segmented replication foci (pseudo-colored in yellow, **panel E**) and for contours (yellow) outlining the small replication foci (**panel F**). The images of panels E and F can be observed in 3-D with red/blue-green viewers.

we have observed the close association of numerous silver grains at numerous sites in early-S-phase. The labeled sites had discrete sizes as evaluated by both area and diameter determinations (Fig. 3). Moreover, the much larger heterochromatin domains that replicate in late-S-phase, and to a lesser extend in mid-S-phase, are actually composed of closely associated labeled foci with virtually identical diameters and areas as the early-S labeled foci (Fig. 3). Pulse-chase experiments demonstrated that the RS labeled in early-S-phase are maintained as similarly labeled clusters of colloidal gold particles later in S-phase and following the next cell generation (Fig. 4).

These findings provide direct evidence at the electron microscopic level for a common size of replication foci throughout the S-phase and their maintenance as fundamental higher order chromatin domains throughout the cell cycle and into subsequent cell generations. Stereologic analysis of labeled electron microscopic sections further demonstrates that the total relative volume occupied by the entire population of RS is virtually identical in early- and mid-S-phases with only a small decrease (approximately 20%) in late-S-phase. Since the average size of the small replication foci is identical throughout S-phase, this implies that the total number of RS at any given time in

S-phase is relatively constant with a small decrease during late-S-phase. Calculation of the total number of RS based on data from early-S-phase and extrapolation to the other periods of S-phase, therefore, provides a reasonable accurate approximation and supports the model of fundamental chromatin domains of ~1 Mbp during DNA replication and throughout the cell cycle [Jackson and Pombo, 1998; Ma et al., 1998; Zink et al., 1998; Berezney, 2002]. Further stereologic studies at the electron microscopic level will be required to directly calculate the number of RS at each period of S-phase and to determine the average amount of DNA present at each chromatin domain.

3-D reconstruction of serial sections enabled a more detailed visualization of these labeled RS. Consistent with previous studies using 3-D confocal microscopy [Wei et al., 1998], we find that the early-S sites form an overall network of association throughout the cell nucleus (Fig. 5). Analysis of the closely associated RS of late-S heterochromatin domains enabled us to better visualize the many individual RS that compose these larger replication foci (Fig. 6).

In summary, the characteristic RS of early-S-phase is demonstrated for the first time at the electron microscopic level. Moreover, late-S heterochromatin is replicated in similar-sized chromatin domains. This leads to the conclusion that replication occurs in similarly-sized RS throughout the S-phase and supports the view that these chromatin domains are universal features of higher order organization and function in the mammalian cell nucleus. 3-D electron microscopic visualization further reveals that the RS during early-S-phase are arranged into higher order networks (Fig. 5). These networks, previously identified following 3-D confocal microscopy and computer image analysis [Wei et al., 1998], have been proposed to form the structural basis for the coordination of DNA replication and transcription programming in the mammalian cell [Berezney and Wei, 1998; Berezney, 2002].

REFERENCES

Berezney R. 2002. Regulating the mammalian genome: The role of nuclear architecture. Adv Enzyme Regul 42: 39–52.

Berezney R, Wei X. 1998. The new paradigm: Integrating genomic function and nuclear architecture. J Cell Biochem Suppl 31:238–242.

Berezney R, Dubey DD, Huberman JA. 2000. Heterogeneity of eukaryotic replicons, replicon clusters, and replication foci. Chromosoma 108:471–484.

Danscher G. 1981. Localization of gold in biological tissue. A photochemical method for light and electron microscopy. Histochemistry 71:81–88.

Dimitrova DS, Berezney R. 2002. The spatio-temporal organization of DNA replication sites is identical in primary, immortalized, and transformed mammalian cells. J Cell Sci 115:4037–4051.

Ferreira J, Paolella G, Ramos C, Lamond AI. 1997. Spatial organization of large-scale chromatin domains in the nucleus: A magnified view of single chromosome territories. J Cell Biol 139:1597–1610.

Fidorra J, Mielke T, Booz J, Feinendegen LE. 1981. Cellular and nuclear volume of human cells during the cell cycle. Radiat Environ Biophys 19:205–214.

Fox MH, Arndt-Jovin DJ, Jovin TM, Baumann PH, Robert-Nicoud M. 1991. Spatial and temporal distribution of DNA replication sites localized by immunofluorescence and confocal microscopy in mouse fibroblasts. J Cell Sci 99:247–253.

Gundersen HJ, Bendtsen TF, Korbo L, Marcussen N, Moller A, Nielsen K, Nyengaard JR, Pakkenberg B, Sorensen FB, Vesterby A, West MJ. 1988. Some new, simple, and efficient stereological methods and their use in pathological research and diagnosis. Apmis 96:379–394.

Hozak P, Hassan AB, Jackson DA, Cook PR. 1993. Visualization of replication factories attached to nucleoskeleton. Cell 73:361–373.

Hozak P, Jackson DA, Cook PR. 1994. Replication factories and nuclear bodies: The ultrastructural characterization of replication sites during the cell cycle. J Cell Sci 107(Pt 8):2191–2202.

Jackson DA, Pombo A. 1998. Replicon clusters are stable units of chromosome structure: Evidence that nuclear organization contributes to the efficient activation and propagation of S phase in human cells. J Cell Biol 140: 1285–1295.

Jaunin F, Visser AE, Cmarko D, Aten JA, Fakan S. 2000. Fine structural in situ analysis of nascent DNA movement following DNA replication. Exp Cell Res 260: 313–323.

Kill IR, Bridger JM, Campbell KH, Maldonado-Codina G, Hutchison CJ. 1991. The timing of the formation and usage of replicase clusters in S-phase nuclei of human diploid fibroblasts. J Cell Sci 100:869–876.

Koberna K, Stanek D, Malinsky J, Eltsov M, Pliss A, Ctrnacta V, Cermanova S, Raska I. 1999. Nuclear organization studied with the help of a hypotonic shift: Its use permits hydrophilic molecules to enter into living cells. Chromosoma 108:325–335.

Leonhardt H, Rahn HP, Weinzierl P, Sporbert A, Cremer T, Zink D, Cardoso MC. 2000. Dynamics of DNA replication factories in living cells. J Cell Biol 149:271–280.

Ma H, Samarabandu J, Devdhar RS, Acharya R, Cheng PC, Meng C, Berezney R. 1998. Spatial and temporal dynamics of DNA replication sites in mammalian cells. J Cell Biol 143:1415–1425.

Malinsky J, Koberna K, Stanek D, Masata M, Votruba I, Raska I. 2001. The supply of exogenous deoxyribonucleotides accelerates the speed of the replication fork in early S-phase. J Cell Sci 114:747–750.

Manders EM, Stap J, Brakenhoff GJ, van Driel R, Aten JA. 1992. Dynamics of three-dimensional replication patterns during the S-phase, analysed by double labelling of DNA and confocal microscopy. J Cell Sci 103:857–862.

Mazzotti G, Rizzoli R, Galanzi A, Papa S, Vitale M, Falconi M, Neri LM, Zini N, Maraldi NM. 1990. High-resolution detection of newly synthesized DNA by anti-bromodeoxyuridine antibodies identifies specific chromatin domains. J Histochem Cytochem 38:13–22.

Nakamura H, Morita T, Sato C. 1986. Structural organizations of replicon domains during DNA synthetic phase in the mammalian nucleus. Exp Cell Res 165:291–297.

Nakayasu H, Berezney R. 1989. Mapping replicational sites in the eucaryotic cell nucleus. J Cell Biol 108:1–11.

Neri LM, Mazzotti G, Capitani S, Maraldi NM, Cinti C, Baldini N, Rana R, Martelli AM. 1992. Nuclear matrix-bound replicational sites detected in situ by 5-bromodeoxyuridine. Histochemistry 98:19–32.

O'Keefe RT, Henderson SC, Spector DL. 1992. Dynamic organization of DNA replication in mammalian cell nuclei: Spatially and temporally defined replication of chromosome-specific alpha-satellite DNA sequences. J Cell Biol 116:1095–1110.

Raska I, Koberna K, Jarnik M, Petrasovicova V, Bednar J, Raska K, Jr., Bravo R. 1989. Ultrastructural immunolocalization of cyclin/PCNA in synchronized 3T3 cells. Exp Cell Res 184:81–89.

Raska I, Michel LS, Jarnik M, Dundr M, Fakan S, Gasser S, Gassmann M, Hubscher U, Izaurralde E, Martinez E. 1991. Ultrastructural cryoimmunocytochemistry is a convenient tool for the study of DNA replication in cultured cells. J Electron Microsc Tech 18:91–105.

Rizzoli R, Baratta B, Maraldi NM, Falconi M, Galanzi A, Papa S, Vitale M, Rizzi E, Manzoli L, Mazzotti G. 1992. DNA synthesis progression in 3T3 synchronized fibroblasts: A high resolution approach. Histochemistry 97: 181–187.

Somanathan S, Suchyna TM, Siegel AJ, Berezney R. 2001. Targeting of PCNA to sites of DNA replication in the mammalian cell nucleus. J Cell Biochem 81:56–67.

Sparvoli E, Levi M, Rossi E. 1994. Replicon clusters may form structurally stable complexes of chromatin and chromosomes. J Cell Sci 107(Pt 11):3097–3103.

van Dierendonck JH, Keyzer R, van de Velde CJ, Cornelisse CJ. 1989. Subdivision of S-phase by analysis of nuclear 5-bromodeoxyuridine staining patterns. Cytometry 10:143–150.

Wei X, Samarabandu J, Devdhar RS, Siegel AJ, Acharya R, Berezney R. 1998. Segregation of transcription and replication sites into higher order domains. Science 281: 1502–1506.

Zink D, Cremer T, Saffrich R, Fischer R, Trendelenburg MF, Ansorge W, Stelzer EH. 1998. Structure and dynamics of human interphase chromosome territories in vivo. Hum Genet 102:241–251.